Interactions of Anesthetics with the Water−Hexane Interface. A Molecular Dynamics Study

Christophe Chipot,[†,§] Michael A. Wilson,[†,‡] and Andrew Pohorille*[,†,‡]

Exobiology Branch, NASA−Ames Research Center, MS 239-4, Moffett Field, California 94035-1000, and Department of Pharmaceutical Chemistry, University of California, San Francisco, San Francisco, California 94143

Received: May 23, 1996; In Final Form: August 26, 1996[⊗]

The free energy profiles characterizing the transfer of nine solutes across the liquid−vapor interfaces of water and hexane and across the water−hexane interface were calculated from molecular dynamics simulations. Among the solutes were *n*-butane and three of its halogenated derivatives, as well as three halogenated cyclobutanes. The two remaining molecules, dichlorodifluoromethane and 1,2-dichloroperfluoroethane, belong to series of halo-substituted methanes and ethanes, described in previous studies (*J. Chem. Phys.* **1996**, *104*, 3760; *Chem. Phys.* **1996**, *204*, 337). Each series of molecules contains structurally similar compounds that differ greatly in anesthetic potency. The accuracy of the simulations was tested by comparing the calculated and the experimental free energies of solvation of all nine compounds in water and in hexane. In addition, the calculated and the measured surface excess concentrations of *n*-butane at the water liquid−vapor interface were compared. In all cases, good agreement with experimental results was found. At the water−hexane interface, the free energy profiles for polar molecules exhibited significant interfacial minima, whereas the profiles for nonpolar molecules did not. The existence of these minima was interpreted in terms of a balance between the free energy contribution arising from solute−solvent interactions and the work to form a cavity that accommodates the solute. These two contributions change monotonically, but oppositely, across the interface. The interfacial solubilities of the solutes, obtained from the free energy profiles, correlate very well with their anesthetic potencies. This is the case even when the Meyer−Overton hypothesis, which predicts a correlation between anesthetic potency and solubility in oil, fails.

Introduction

Although the phenomenon of general anesthesia has been known for over a century, the site and mechanism of anesthetic action remain unknown. For many years, the thinking about this phenomenon has been significantly influenced by the Meyer−Overton hypothesis. This hypothesis predicts a correlation between the potency of inhaled anesthetics and their lipophilicity, *i.e.*, solubility in a hydrophobic phase (*e.g.*, olive oil), considered as a model for the interior of the membrane.[1,2] Since anesthetics rapidly equilibrate across all cellular compartments,[3] their equilibrium properties, such as solubility, are relevant to the mechanism of their action. For conventional anesthetics, the observed correlation is remarkably accurate over several orders of magnitude of anesthetic potencies and for different animals.[4] The success of the Meyer−Overton hypothesis led to the suggestion that the site of anesthetic action might be located inside the lipid bilayer of neuronal tissue.[5] In this environment, anesthetics would act either by disrupting the lipid bilayer or by interacting with receptor sites buried in the membrane.

If, however, the Meyer−Overton hypothesis is tested on a broader range of potentially anesthetic compounds, the correlation between potency and lipophilicity is markedly less convincing. In particular, some halogenated hydrocarbons that are predicted to be good anesthetics from the Meyer−Overton hypothesis exhibit no anesthetic activity (nonanesthetics),[6−9] and several other compounds show an anesthetic potency that is much weaker than predicted (transitional compounds).[7] All these compounds have very low solubilities in water. In contrast, alkanols, which are highly soluble in water, appear to be more potent anesthetics than expected from the Meyer−Overton hypothesis.[10] These results indicate that anesthetic potencies cannot be fully predicted from solubilities in oil alone. In particular, some level of solubility in water appears to be required for anesthetic action.

These recent discoveries suggest that the anesthetic potency might correlate better with the solubility at the interface between water and a nonpolar phase than with the solubility in oil. This paper is devoted to testing this idea. Since interfacial solubility is very difficult to measure experimentally, molecular dynamics simulations were employed to calculate this quantity at the water−hexane interface. In this work, we study two series of molecules of structurally similar halogenated compounds, each ranging from potent anesthetics to nonanesthetics. In the first series, *n*-butane, a weak anesthetic, and 1,1,2,2,3,3,4,4-octafluorobutane, a known anesthetic, are compared with the nonanesthetic 2,3-dichloroperfluorobutane [(*R*,*R*)-enantiomer] and the transitional 1,2,3,4-tetrachloroperfluorobutane [(*S*,*S*)-enantiomer]. The second series consists of cyclobutane derivatives: 1-chloro-1,2,2-trifluorocyclobutane, 1,2-dichloroperfluorocyclobutane,[11] and perfluorocyclobutane. The first of these compounds is an anesthetic, whereas the remaining are not. In addition, we study the anesthetic dichlorodifluoromethane and the transitional 1,2-dichloroperfluoroethane. These two molecules are structurally closely related to fluorinated methanes and ethanes, the transfer of which across the water−hexane and water−membrane interfaces has been studied previously.[12,13]

[†] NASA−Ames Research Center.
[‡] University of California.
[§] On leave from: Laboratoire de Chimie Théorique, Unité de Recherche Associée au CNRS No. 510, Université Henri Poincaré-Nancy I, BP. 239, 54506 Vandoeuvre-lés-Nancy Cedex, France.
[⊗] Abstract published in *Advance ACS Abstracts,* December 1, 1996.

S1089-5647(96)01513-1 CCC: $14.00

Our approach consists of four steps. First, potential energy functions for the molecules of interest are developed. Second, the free energy profiles describing the transfer of these molecules across the liquid−vapor interfaces of both water and hexane are calculated. From these profiles, solubilities of the solutes in water and in hexane are determined and compared with experimentally measured solubilities to ascertain the accuracy of our calculations. Next, the free energy profiles describing the transfer of the solutes across the water−hexane interface are calculated. Finally, these profiles are used to determine the interfacial solubilities and to correlate them with anesthetic potencies.

Methods

A. Description of the System. The pure water system consisted of 490 molecules arranged in a lamella of the liquid phase with vapor above and below. Thus, the system contained two liquid−vapor interfaces. The same arrangement was used for the system of 82 hexane molecules. In the water−hexane system, a lamella of liquid water was in contact with a lamella of liquid hexane. This system consisted of 484 water molecules and 83 hexane molecules. In addition to a water−hexane interface, it also contained a liquid−vapor interface of water and a liquid−vapor interface of hexane.

The dimensions of all three systems were 24×24 Å^2 in the xy plane of the interface and 150 Å in the z dimension perpendicular to the interface. Periodic boundary conditions were applied in all three directions. The average widths of the lamellae of water, hexane, and water−hexane were 26, 33, and 58 Å, respectively.

B. Potential Energy Functions. The potential energy function, H_{total}, used to describe both the intra- and intermolecular interactions in the system is a sum of individual contributions arising from bond stretching and deformation of valence and torsional angles as well as Lennard-Jones and Coulomb interactions between nonbonded atoms:

$$H_{\text{total}}(\mathbf{r}) = \sum_{\text{bonds}} k_r(r - r_0)^2 + \sum_{\text{angles}} k_\theta(\theta - \theta_0)^2 + \sum_{\text{dihedrals}} \sum_{n=1}^{n=3} V_n[1 + \eta \cos(n\phi - \phi_0)] + \sum_{i<j} \left[\frac{A_{ij}}{R_{ij}^{12}} - \frac{B_{ij}}{R_{ij}^{6}} + \frac{q_i q_j}{R_{ij}} \right] \quad (1)$$

where k_r, r, and r_0 are the bond stretching constant, the bond length, and the equilibrium bond length, respectively; k_θ, θ, and θ_0 are the valence angle stretching constant, the valence angle, and the equilibrium valence angle, respectively; V_n is the coefficient of the Fourier series describing the dihedral ϕ, ϕ_0 is the phase, n is the periodicity of the torsional term, and $\eta = 1$, -1, and 1 for $n = 1$, 2, and 3, respectively; R_{ij} is the interatomic distance between atoms i and j, A_{ij} and B_{ij} are the Lennard-Jones nonbonded repulsion and attraction coefficients, respectively, and q_i is the net atomic charge on atom i; $\mathbf{r}$ represents the full set of intramolecular coordinates of the solute molecule.

Water molecules were represented by the TIP4P model.[14] Hexane molecules were described by the OPLS potential functions.[15,16] In this description, the aliphatic CH_n groups were treated as electrically neutral united atoms, the total mass of which was centered on the carbon atoms. In molecular dynamics simulations, the bond lengths and the valence angles of both water and hexane were constrained to their equilibrium values, using the SHAKE algorithm.[17,18] The water−hexane Lennard-Jones parameters were obtained from standard OPLS combination rules.[15]

TABLE 1: Lennard-Jones Parameters Used in the Molecular Simulations

nonbonded atoms[a,b]			
i	j	A_{ij} (kcal Å^{12}/mol)	B_{ij} (kcal Å^6/mol)
C	OW	574 670.000	601.359 985 35
C	C2	2 328 200.000	1098.699 951 17
C	C3	2 540 300.000	1198.800 048 83
H	OW	40 179.000	101.599 998 47
H	C2	140 970.000	160.750 000 00
H	C3	153 810.000	175.389 999 39
F	OW	305 190.000	362.209 991 46
F	C2	1 339 800.000	606.940 002 44
F	C3	1 461 800.000	662.219 970 70
Cl_1	OW	1 561 300.000	1339.300 048 83
Cl_1	C2	5 124 200.000	1982.300 048 83
Cl_1	C3	5 591 000.000	2162.800 048 83
Cl_2	OW	1 561 300.000	1339.300 048 83
Cl_2	C2	3 571 200.000	1381.500 000 00
Cl_2	C3	3 896 500.000	1507.300 048 83

[a] See Figure 1. [b] OW = TIP4P water[14] oxygen; C2 = OPLS[15,16] methylene carbon; C3 = OPLS methyl carbon.

The intramolecular parameters k_r, r_0, k_θ, and θ_0 were taken from the AMBER force field.[19,20] The Lennard-Jones parameters, listed in Table 1, were previously optimized in a series of calculations[12,21] to reproduce experimentally measured solubilities of methane, fluoromethane, difluoromethane, trifluoromethane, perfluoromethane, and chloromethane in water and hexane, and dichlorodifluoromethane in hexane. Those calculations were performed using the particle insertion method of Widom.[22] This method is both fast and accurate, since a large number of statistically representative solute−solvent configurations can be generated simply from configurations of the neat solvent. This high efficiency allowed us to explore a broad range of parameter values.

We started our search for the most suitable set of parameters with the AMBER values of Gough *et al.*[23] These parameters were chosen to describe the thermodynamic properties of liquid fluoromethanes correctly. The atomic charges were derived to reproduce quantum mechanical electrostatic potentials around the solutes. In all cases, the charges on fluorine atoms were close to -0.2 ecu (electronic charge unit). Unfortunately, the AMBER parameters were not sufficiently accurate to reproduce experimental free energies of solvation of fluoromethanes in water and in hexane (the root-mean-square deviation was 0.6 kcal mol^{-1}). These parameters were, therefore, modified so that they yielded accurate solubilities in hexane (electrostatic solute−solvent interactions are absent from the OPLS model of oil). However, application of the modified parameters with the standard combination rules for calculating solubilities in water did not produce satisfactory results. This failure forced us to depart from using the combination rules and apply different parameters describing interactions of fluoromethanes with water and hexane. The observed difficulty is not unique to this study. It has been shown, for example, that the interaction potentials constructed using combination rules do not reproduce the experimental surface tension between water and decane[24] and do not yield correct solubilities of water in a membrane.[25] Although, in general, abandoning combination rules is undesirable because it might require fitting a large number of parameters, it was necessary here to ensure the accuracy needed for the success of this study.

Point charges on atoms of the solutes were obtained from quantum-mechanical calculations. Except for the halo-substi-

TABLE 2: Conformations Used To Generate the Net Atomic Charges

molecule[a]	conformation[b]	ΔE (kcal/mol)	μ (D) DFT (DZVPD[31])	μ (D) reproduced[c]
$C_2F_4Cl_2$ (**b**)	*anti*	0.000	0.000	0.000
	gauche	1.150	0.675	0.651
C_4H_{10} (**f**)	*anti*	0.000	0.000	0.001
	gauche	1.052	0.101	0.107
	eclipsed	3.249	0.073	0.080
$C_4H_2F_8$ (**g**)	*g*−*a*−*a*	0.000	2.321	2.403
	g−*g*−*a*	0.719	2.400	2.484
	g−*e*−*a*	3.234	2.356	2.444
$C_4F_8Cl_2$ (**h**)	*anti*	0.000	0.947	0.903
	gauche	0.001	0.832	0.880
	eclipsed	2.454	0.581	0.452
$C_4F_6Cl_4$ (**i**)	*a*−*a*−*a*	0.000	0.782	0.770
	a−*g*−*a*	0.275	0.712	0.694
	g−*a*−*a*	0.445	0.160	0.214
	a−*e*−*a*	5.574	0.389	0.353

[a] See Figure. [b] *a* = antistaggered, *g* = gauche-staggered, and *e* = eclipsed. [c] From the set of multiconformational point charges.

tuted cyclobutanes, the geometries of the anesthetic compounds were first optimized from density functional theory (DFT) calculations in the local spin density (LSD) approximation, using the DGAUSS program,[26] and a DZVP basis set.[27] The GAUSSIAN 92/DFT[28] suite of programs was subsequently employed to compute the molecular electrostatic potential of the energy-minimized structures, with a self-consistent inclusion of nonlocal gradient corrections to the functional, as introduced by Becke[29] and Perdew.[30] These calculations were performed using a DZVPD basis set,[31] in which the d exponents for chlorine were optimized from small chlorine-containing molecules. Net atomic charges were then derived to reproduce the quantum-mechanically calculated electrostatic potential, using the GRID program.[32] For flexible solutes (*viz*. ethanes and butanes), between two and four conformers were considered to carry out a multiconformational fit[33,32] of the point charges to the DFT molecular electrostatic potential. The calculated relative energies and dipole moments of these conformers are given in Table 2. For the three halo-substituted cyclobutanes, the geometry was determined from *ab initio* calculations at the HF/6-31+G* level,[34] using GAUSSIAN 92/DFT, and the sets of point charges were fitted to the MP2/6-311++G** molecular electrostatic potential. The point charges on atoms for all solutes studied in this work are shown in Figure 1.

It should be noted that, in some cases, halogen atoms were assigned positive partial charges. This is in contradiction with "chemical intuition" in the sense that the charges assigned to neighboring atoms do not reflect the anticipated differences in electronegativities between them. This is known to be especially the case for weakly polar species, like many of those discussed in this paper, and has been previously discussed in the literature.[35,36] This departure from "chemical intuition" is, at least in part, due to representing the electrostatic energy by the sum of atom−atom Coulomb terms only. Then, the effect of higher local multipoles may considerably modulate the derived effective atomic charges. In addition, we note that the counterintuitive charges obtained in the series of alkyl halides are not artifacts of the level of theory employed in our calculations. If the atomic charges on dichlorodifluoromethane are fitted to the MP2/6-31++G** molecular electrostatic potential, instead of the Becke3P86/DZVPD, the charges on fluorine and chlorine are 0.072 and 0.113 ecu, respectively.

The procedure employed to design force fields for halogenated hydrocarbons, which involves Lennard-Jones parameters derived for halogenated methanes together with atom-centered potential derived partial charges, is a consistent and a well-

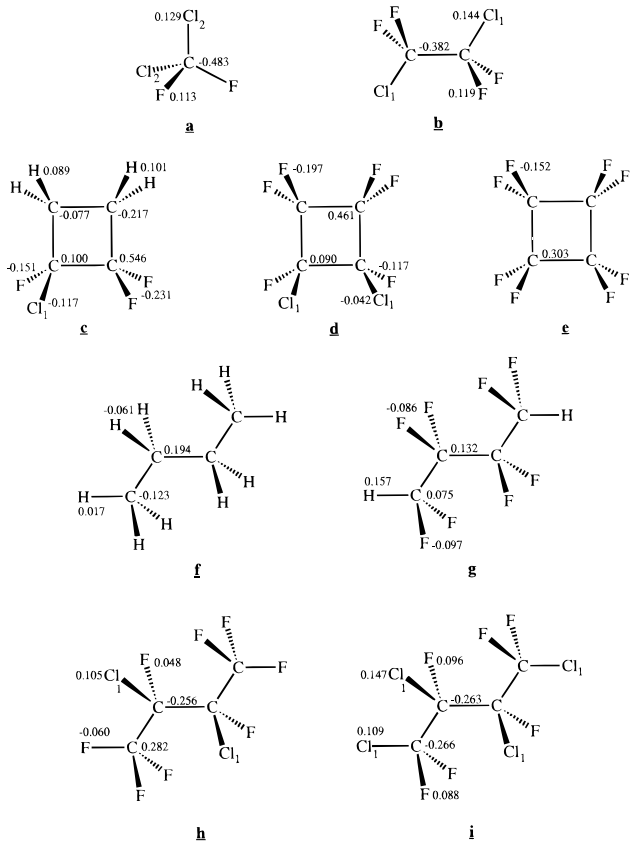

Figure 1. Electrostatic potential derived charges of dichlorodifluoromethane (**a**), 1,2-dichloroperfluoroethane (**b**), 1-chloro-1,2,2-trifluorocyclobutane (**c**), 1,2-dichloroperfluorocyclobutane (**d**), perfluorocyclobutane (**e**), *n*-butane (**f**), 1,1,2,2,3,3,4,4-octafluorobutane (**g**), 2,3-dichloroperfluorobutane (**h**), and 1,2,3,4-tetrachloroperfluorobutane (**i**).

defined one. More importantly, as will be shown below, it is reliable for predicting the solubilities of these compounds in water and oil, an essential requirement in this work. This procedure, however, does not appear to yield intuitive, all-purpose potential functions that are likely to reproduce accurately a broad range of properties of halogenated hydrocarbons. Developing such functions would be of great utility but might prove to be a difficult task. As discussed above, the fluoromethanes provide a relevant example. The parameters yielding a good equation of state[23] do not reproduce well the free energies of solvation, and conversely, the parameters which give accurate solubilities in water and oil are not optimal for describing the pure liquid state.

C. Molecular Dynamics Simulations. The molecular dynamics equations of motion were integrated using the Verlet algorithm.[37] Different time steps were used depending upon the location of the solute molecule with respect to the solvent interface. When the solute was on the vapor side of the liquid−vapor interfaces of water or hexane, an integration time step of 1 fs was used; this was increased to 2−2.5 fs when the solute was inside the liquid phase. The average temperature of the system was 310 K, equal to the temperature at which anesthetic potencies of the solutes were measured. All the simulations were carried out using the COSMOS[38] program.

Both the hexane molecules and the anesthetic solutes were divided into electrically neutral subunits for the evaluation of intermolecular interactions.[39] One of the atoms within each subunit was selected to be the central atom of that subunit. The potentials were truncated smoothly, using a switching function[40] at separations from 7.5 to 8.0 Å between the selected central atoms of the subunits and/or the oxygen atoms of water.

Each free energy profile for the transfer of an anesthetic solute across the water−hexane interface, or the liquid−vapor interface of water or hexane, was obtained from a series of simulations in which the solute was moved along the z direction in sequentially overlapping ranges, or "windows". The "umbrella sampling" approach[41−43] was employed. In each window, the solute was confined to a predefined range, $z_{min} < z < z_{max}$, by a harmonic restraining potential, $k(z - z_{min})^2$ for $z < z_{min}$ and $k(z_{max} - z)^2$ for $z > z_{max}$. The total distance by which the solutes moved along the z direction varied between 20 and 25 Å, depending on the interface. Typically, four to six windows 6 Å wide were needed to cover this distance. Consecutive windows overlapped by at least 1.5 Å. In each window, the free energy of the solute $A(z)$ was estimated from $P(z)$, the probability of finding the solute at position z:

$$A(z) = -k_B T \ln P(z) \tag{2}$$

where k_B is the Boltzmann constant and T is the temperature of the system. The complete free energy profiles were generated by superimposing the curves of $A(z)$ obtained from individual windows and requiring that $A(z)$ be a continuous function of the z coordinate. This was done using the weighted histograms analysis method (WHAM).[44]

The molecular dynamics trajectory for each window varied from 0.5 to 1.0 ns, depending on the quality of the statistical data for $P(z)$, and the total length of the trajectories used for obtaining the full free energy profile for a given solute was between 3 and 5 ns. The statistical error in each window was estimated by treating $A(z_{max}) - A(z_{min})$, obtained from 0.1 ns segments of the trajectory, as independent measurements. In addition, the root-mean-square deviations of fitting the free energies from two consecutive windows in the overlapping regions, weighted by the number of data points in each overlapping bin (not required in WHAM), was calculated. To estimate the uncertainty in calculating the free energy difference between the end points of the full free energy profile, the uncertainties from the individual windows and the overlaps between windows were considered as independent contributions.

To improve equilibration between stable conformations of flexible solutes, biasing potentials, $U_{bias}(\phi)$, that depend on the values of torsional angles in the solute molecules were added to the force field. These potentials were empirically designed to lower the energy barriers between different conformations in the gas phase. The estimated free energies were subsequently unbiased to correct for this modification.[45] All conformations predicted to be of low energy were sampled during the simulations in the different environments.

Under equilibrium conditions, in the limit of infinite dilution, the changes of the free energy along z can be related to the corresponding changes in concentration:

$$c(z)/c_b = e^{-\Delta A(z)/k_B T} \tag{3}$$

where $c(z)$ and c_b are concentrations of the solute at z and in a bulk phase (gas phase, liquid water, or liquid hexane), respectively, and $\Delta A(z)$ is the free energy difference between the solute at position z and in the same bulk phase. For the liquid−vapor interfaces of water and hexane, the difference between the end points of the free energy profile for a given solute yields its Ostwald solubility (the ratio of the equilibrium concentration of the solutes dissolved in the solvent and the concentration of this solute in the gas phase, measured under 1.0 atm and at a temperature T) in the bulk liquid phase.

TABLE 3: Free Energies of Solvation of the Anesthetic Solutes in Water and Hexane

	water		hexane		water/hexane		
molecule[a]	calc	exp	calc	exp[b]	calc	exp	calc (w/h)[c]
CF_2Cl_2 (**a**)	1.7	1.91[d]	−0.4	−0.47	2.0	2.38	2.1
$C_2F_4Cl_2$ (**b**)	3.2	2.67[d]	−1.8	−2.15	4.4	4.82	5.0
$C_4H_4F_3Cl$ (**c**)	−0.3	−0.28[d]	−3.8	−3.55	3.3	3.27	3.5
$C_4F_6Cl_2$ (**d**)	2.7	2.73[d]	−3.4	−3.25	6.6	5.98	6.1
C_4F_8 (**e**)	3.6	3.95[d]	−1.5	−1.20	5.4	5.15	5.1
C_4H_{10} (**f**)	2.2	2.48[e]	−3.2	−2.53	5.7	5.01	5.4
$C_4H_2F_8$ (**g**)	2.0	1.13[e]	−2.8	−2.07	4.6	3.20	4.8
$C_4F_8Cl_2$ (**h**)	4.2	3.96[d]	−3.1	−3.17	6.9	7.14	7.3
$C_4F_6Cl_4$ (**i**)	2.2	2.35[b]	−3.8	−3.35	6.3	5.70	6.0

[a] See Figure 1. [b] Unpublished results provided by E. I. Eger. [c] Calculated from the individual simulations at the water−vapor and hexane−vapor interfaces. [d] Reference 7. [e] Reference 48.

Results and Discussion

A. Interactions of Anesthetics with the Liquid−Vapor Interface of Water. The excess free energies, $\Delta A_{exc}(z)$, as a function of the position of the anesthetic compounds along the z coordinate, perpendicular to the water−air interface, are shown in Figure 2. $\Delta A_{exc}(z)$ is defined as the quasi-static work required to bring the center of mass of the solute from the gas phase to the position z. The values at the end points on the water side of the excess free energy profiles, approximately 10 Å from the interface, yield the free energies of dissolving the solutes in water. These values are listed in Table 3 and compared with the free energies obtained from Ostwald solubilities measured at the same temperature.[46] As can be seen from this table, the calculated hydration free energies agree well with the corresponding experimental values. Only for two molecules, 1,2-dichloroperfluoroethane and 1,1,2,2,3,3,4,4-octafluorobutane, did the discrepancy between the calculated and the experimental hydration free energies exceed 0.35 kcal/mol. The root-mean-square deviation of the calculated free energies from the experimental values is 0.3 kcal/mol. A similar accuracy was obtained for other, previously studied, anesthetic molecules.[12,13] This deviation is also close to the statistical uncertainties calculated for the free energies of hydration, which vary for different molecules between 0.3 and 0.4 kcal/mol.

All the free energy profiles displayed in Figure 2 exhibit minima near the water surface. Thus, all the solutes are surface active; *i.e.*, their concentrations are higher at the surface than in the bulk water. The depth of the interfacial minima in $\Delta A_{exc}(z)$ varies between 1 and 3 kcal/mol. As we have shown previously,[12] these minima can be interpreted as arising from a superposition of two monotonically, but oppositely, changing contributions to the free energy. As the solute moves from the gas phase to liquid water, favorable contributions to the free energy from electrostatic and van der Waals solute−solvent interactions increase. Once the solute approaches the surface, these favorable terms are partially balanced by an unfavorable contribution to the free energy due to the quasi-static work needed to form a cavity in the liquid that is capable of accommodating the solute. This contribution increases across the interface until the solute becomes fully immersed in water. This interpretation leads to the conclusion that, among structurally similar solutes, those that are more polar (*i.e.*, more soluble in water and possessing a larger permanent dipole moment) should exhibit deeper interfacial minima. As can be seen in Figure 2, this is indeed the case.

The accuracy of the calculated free energy profiles can be assessed by relating them to experimentally measurable thermodynamic functions of adsorption. The surface excess concentration of an ideal dilute solution, Γ_s, under isothermal

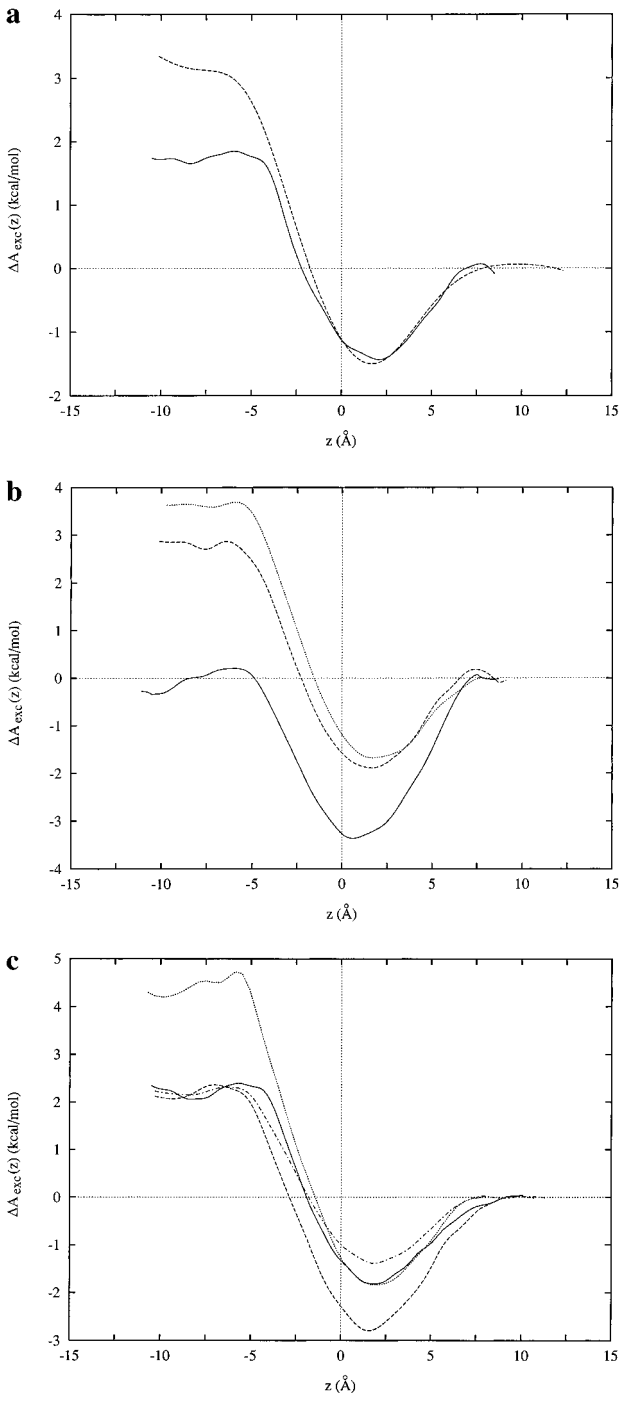

Figure 2. Free energy profiles for transferring the solutes across the water liquid−vapor interface: (a) dichlorodifluoromethane (solid line) 1,2-dichloroperfluoroethane (dashed line), (b) 1-chloro-1,2,2-trifluorocyclobutane (solid line), 1,2-dichloroperfluorocyclobutane (dashed line), perfluorocyclobutane (dotted line), (c) *n*-butane (solid line), 1,1,2,2,3,3,4,4-octafluorobutane (dashed line), 2,3-dichloroperfluorobutane (dotted line), and 1,2,3,4-tetrachloroperfluorobutane (dot-dashed line). The origin, $z = 0$, is at the equimolar surface of water. The vapor phase is located at $z > 0$, and the liquid phase at $z < 0$.

conditions, can be expressed as a function of the surface tension, γ, and bulk concentration of solute in the liquid phase, c_l, *via* the Gibbs adsorption isotherm:

$$\Gamma_s = -\frac{c_l}{k_B T}\frac{\partial \gamma}{\partial c_l} \qquad (4)$$

Consequently, it is possible to determine experimentally the surface excess concentration from measurements of surface tension as a function of concentration.

The surface excess of solute can be calculated directly from the molecular dynamics simulation by converting the free energy profile to the concentration profile, using eq 3, and integrating across the interface:

$$\Gamma_s = \int_0^{z_{Gibbs}} [c(z) - c_g]\, dz + \int_{z_{Gibbs}}^{L_z/2} [c(z) - c_l]\, dz \qquad (5)$$

where c_g is the concentrations in the gaseous phase, c_l was defined in eq 4, L_z is the length of the box in the direction perpendicular to the interface, $z = 0$ is at the center of the water lamella, and z_{Gibbs} is the position of the equimolar surface of the solvent defined as the position where the surface excess of solvent vanishes. This was determined from eq 5, using the water density profile.

At low solute concentrations, the surface excess is a linear function of the concentration, and it is convenient to compare the experimental and molecular dynamics results for the limiting slope of the surface excess *versus* concentration curves and to use the partial pressure of solute over the interface, P_s as the concentration variable.

Unfortunately, experimental studies of the change of the water surface tension in the presence of applied pressures of hydrocarbons or halo-substituted hydrocarbons are relatively scarce; we have found data only for *n*-butane. From their experimental study of the surface tension of water in equilibrium with compressed *n*-butane, Jho *et al*. found a limiting slope of the "Γ_2 *versus* P_s" isotherm equal to 4.73×10^{13} molecules cm^{-2} atm^{-1} at 310 K. Hauxwell *et al* have examined the adsorption of a series of four normal alkanes (*viz*. C_5 to C_8) on water and observed a roughly linear change of the free energy of adsorption with respect to the number of carbon atoms in the alkane. In fact, the plots characterizing the variation of the enthalpy and the entropy of adsorption with respect to the length of the aliphatic chain have slightly different slopes depending on whether the number of carbon atoms is odd or even. The surface tension of water was measured under low pressures of saturated hydrocarbons (*i.e*., typically $P_s \leq 0.2$ atm), thus ensuring a reliable estimate of the limiting slope. A straightforward extrapolation to *n*-butane at 310 K of the C_5 and C_7 data of Hauxwell *et al*. gives a slope equal to 0.83×10^{13} and 0.73×10^{13} molecules cm^{-2} atm^{-1} from the C_6 and C_8 data. The origin of the difference between the experimental results has not been unequivocally established.

For *n*-butane, the molecular dynamics results yield a limiting slope of 1.70×10^{13} molecules cm^{-2} atm^{-1}. This number lies between the two experimental results and differs from either of these results by only a factor of 3.

B. Interactions of Anesthetics with the Hexane−Air Interface. The calculated free energies of solvating the anesthetic solutes in hexane, listed in Table 3, are in a good agreement with experimental values determined from measured Ostwald solubilities.[46] Only two values, the solubilities of *n*-butane and 1,1,2,2,3,3,4,4-octafluorobutane, are inaccurate by more than 0.4 kcal/mol, and the root-mean-square deviation between the calculated and experimental free energies of solvation in hexane is the same as the deviation calculated previously for liquid water.

In contrast with the free energy profiles for transferring the anesthetics across the liquid−vapor interface of water, the profiles across the liquid−vapor interface of hexane either decrease monotonically toward hexane or have very shallow interfacial minima. Examples of such profiles are shown in Figure 3. The interfacial behavior of the solutes is determined by the increasingly attractive van der Waals interactions between the solute and the solvent. If this behavior is again considered

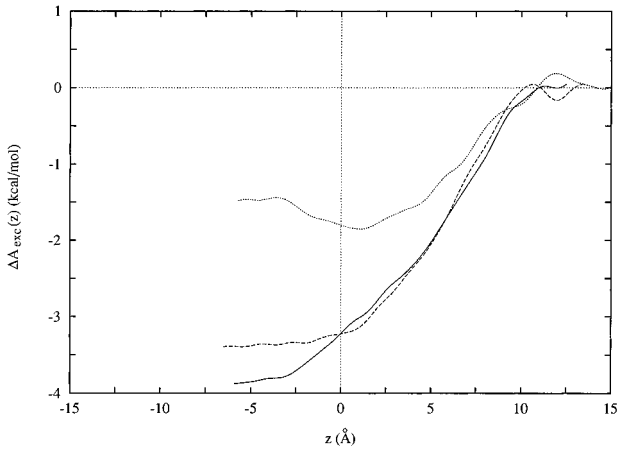

Figure 3. Free energy profiles for transferring 1-chloro-1,2,2-trifluorocyclobutane (solid line), 1,2-dichloroperfluorocyclobutane (dashed line), and perfluorocyclobutane (dotted line), across the hexane liquid−vapor interface: The origin, $z = 0$, is at the equimolar surface of hexane. The vapor phase is located at $z > 0$, and the liquid phase at $z < 0$.

in terms of a balance between contributions to $\Delta A_{exc}(z)$ from solute−solvent interactions and the work of cavity formation, the absence of interfacial minima can be explained by observing that the reversible work of forming molecular-sized cavities is markedly smaller in hexane than in water.[47]

C. Interactions of Anesthetics with the Water−Hexane Interface. The free energy profiles across the water−hexane interface for all nine solutes are shown in Figure 4.[48] The differences between the end points on the water and on the hexane sides of the profiles yield the free energies of transferring the solutes from hexane to water. These free energies are listed in Table 3, where they are compared with the same quantities calculated as differences between the solvation free energies in water and hexane, obtained either from the measured Ostwald solubilities or from the molecular dynamics simulations reported above. The comparison with the experimental values provides a measure of accuracy of the calculated free energies of transfer. Generally, the agreement between the calculated and experimental free energies is good. Only for 1,1,2,2,3,3,4,4-octafluorobutane is the experimental values not well reproduced. The comparison between the free energy of transfer calculated directly and indirectly (from solvation free energies) tests the consistency of our results. In the absence of statistical uncertainties, both methods should yield identical results. As can be seen from Table 3, discrepancies not exceeding ±0.6 kcal/mol are observed. This is expected, considering that the solvation free energies and the directly calculated free energies of transfer have statistical uncertainties of 0.3−0.4 kcal/mol each.

All the free energy profiles in Figure 3 exhibit interfacial minima. Their depths are related to the polarities of the solute molecules. The most polar molecules in the series 1,1,2,2,3,3,4,4-octafluorobutane and 1-chloro-1,2,2-trifluorocyclobutane have interfacial minima approximately 1.5 kcal/mol deep and should therefore be considered as interfacially active. In contrast, the minima for nonpolar solutes are very shallow, small compared to the thermal energy $k_BT \approx 0.6$ kcal/mol. These molecules are not expected to exhibit interfacial activity. Exactly the same pattern was observed previously for other molecules of anesthetic interest: methane, fluoromethanes,[12] and fluoroethanes.[13] For methane and its fluorinated derivatives, $\Delta A_{exc}(z)$ across the water−hexane interface was partitioned into electrostatic and nonelectrostatic contributions. The electrostatic term decreases monotonically during transfer from the nonpolar solvent (hexane) to the polar medium (water). The nonelectrostatic term,

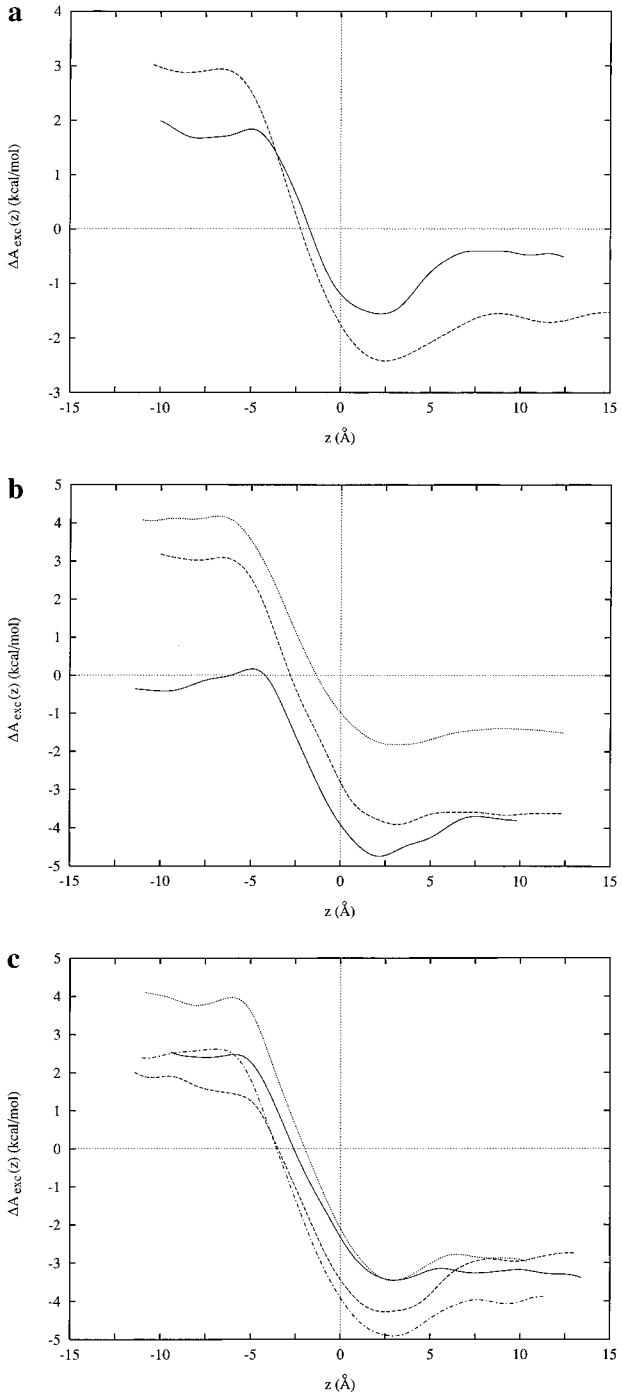

Figure 4. Free energy profiles for transferring the solutes across the water−hexane interface: (a) dichlorodifluoromethane (solid line) 1,2-dichloroperfluoroethane (dashed line), (b) 1-chloro-1,2,2-trifluorocyclobutane (solid line), 1,2-dichloroperfluorocyclobutane (dashed line), perfluorocyclobutane (dotted line), (c) *n*-butane (solid line), 1,1,2,2,3,3,4,4-octafluorobutane (dashed line), 2,3-dichloroperfluorobutane (dotted line), and 1,2,3,4-tetrachloroperfluorobutane (dot-dashed line). The origin, $z = 0$, represents the interface. The hexane phase is located at $z > 0$, and the aqueous phase at $z < 0$.

dominated by the free energy of cavity formation, exhibits an opposite behavior—it increases as the solute is transferred from hexane to water. For polar molecules, the balance between these two types of interactions yields appreciable interfacial minima in the free energy. For nonpolar solutes, the electrostatic term contributes only slightly to $\Delta A_{exc}(z)$, and therefore, interfacial minima are very weak. Although we have not performed a similar partitioning of the free energy in this work, similarities to the previously reported free energy profiles suggest that the

profiles in Figure 3 can be interpreted in exactly the same manner. We note that none of the polar compounds studied here have well-separated hydrophobic and hydrophilic parts and, therefore, cannot be considered an amphiphile. This considerably broadens the conventional picture of interfacial activity in which only amphiphilic molecules, capable of simultaneously burying their hydrophilic portions in water and exposing the hydrophobic parts to a nonpolar phase, can be interfacially active.

The free energy profiles at the water−hexane interface bear some resemblance to the profiles across the liquid−vapor interface of water. In both cases, the free energies exhibit interfacial minima that increase with solute polarity. However, the minima at the water−hexane interface are not as deep as those at the liquid−vapor interface of water. In both cases, the electrostatic contribution to the free energy is very similar. However, the nonelectrostatic term decreases more sharply going from water to hexane than from water to vapor due to solute−hexane van der Waals interactions. The net result is that the end points of the free energy curves in hexane are lower than in water vapor and that the minima at the interface are shallower.

The presence of the interface can affect the orientational preferences of solute molecules. In bulk water and in hexane, all orientations of the solutes are equally probable. Near the interface, however, polar molecules might adopt preferential orientations due to favorable interactions between their charge distributions and the excess electric field created by the solvent. This electric field arises mostly from a slight asymmetry in the orientational distribution of water molecules located in the anisotropic interfacial environment.[49−51] For most solutes presented here, the effect of the interface on the molecular orientations is only minor, because their dipole moments are generally small (see Table 2). One clear exception is 1,1,2,2,3,3,4,4-octafluorobutane, which has the largest permanent dipole moment among the studied molecules (2.32 D in the lowest energy, *anti* conformation). At the interface, this solute exhibits a tendency to align its dipole with the excess interfacial electric field pointing in the *z* direction toward liquid water. Such a preference is expected from the first-order (linear) perturbation theory and was previously observed for another polar solute, 1,1,2-trifluoroethane.[13] This preference, however, does not appear to be universal. For some small, dipolar solutes, orientations parallel to the interface dominate due to the large fluctuations of the instantaneous electric field in this direction.[12] This is a nonlinear (second order) effect in the electric field.

The transfer of flexible solutes across an interface separating liquids of very different polarity can have a considerable influence on the conformational equilibria of these molecules. The previously studied examples are 1,2-dichloroethane[52] and 1,1,2-trifluoroethane.[13] In both cases, the most stable conformation in the gas phase (*anti* and *gauche*, respectively) has a very small permanent dipole moment or none at all. This conformation is also preferred in hexane. However, as the solute moves to water, the conformational equilibrium progressively shifts toward another low-energy conformation (*gauche* and *anti*, respectively) that possesses a significantly larger dipole moment. For the molecules studied here, no significant shifts in conformational equilibria are observed because low-energy conformations of each solute have similar dipole moments (see Table 2).

D. Relationship between Interfacial Activity and Anesthetic Action. According to the Meyer−Overton hypothesis, the potency of anesthetic compounds should correlate with their solubility in a lipidlike phase, *e.g.*, olive oil. One measure of anesthetic potency is the maximum alveolar concentration (MAC). MAC is defined as an average applied partial pressure of an anesthetic that suppresses movement of animals in response to a noxious stimulus. Lower values of MAC correspond to higher anesthetic potencies. Then, based on the Meyer−Overton relationship, it is predicted that the product of MAC and the solubility in olive oil,[53,7] s_{oil}, for different anesthetics should be a constant, independent of the solubilities of these compounds in water. This product for anesthetics studied in this work and in our previous studies[12,13] is shown in Figure 5, and the corresponding MAC values for the compounds considered here are listed in Table 4. Although most compounds obey the Meyer−Overton relationship, there are two clear exceptions—1,2,3,4-tetrachloroperfluorobutane and 1,2-dichloroperfluoroethane are markedly less potent than predicted from this relationship. These molecules are examples of transitional compounds. If hexane is used as a model lipidlike phase rather than olive oil, the overall agreement with the Meyer−Overton hypothesis becomes worse.

To explain the observed deviations we consider an analog of the Meyer−Overton hypothesis in which solubilities at the water−hexane interface are used instead of solubilities in oil. Interfacial solubilities, s_{int}, are defined as

$$s_{int} = C \int_{z_1}^{z_2} e^{-\Delta A_{exc}(z)/kT}\, dz \qquad (6)$$

and depend, in general, on the definition of the interfacial range $[z_1,z_2]$. Here, C is a constant that allows for choosing the desired units of s_{int}.

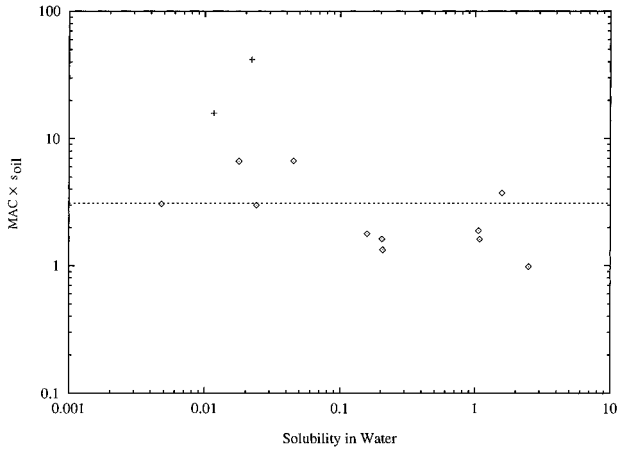

Figure 5. Product of the measured anesthetic partial pressure, MAC, and the solubility in oil *versus* the solubility in water for 13 anesthetics (*i.e.*, seven compounds studied here and six previously studied compounds belonging to the series of halo-substituted methanes and ethanes). Transitional compounds are marked by crosses (+) and the anesthetics that obey the Meyer−Overton hypothesis by diamonds (◇).

TABLE 4: Maximum Alveolar Concentrations (MAC) of the Anesthetics

molecule[a]	MAC
CF_2Cl_2 (**a**)	1.1[b]
$C_2F_4Cl_2$ (**b**)	1.27[b]
$C_4H_4F_3Cl$ (**c**)	0.0153[b]
$C_4F_6Cl_2$ (**d**)	N.A. (0.25)[b,c]
C_4F_8 (**e**)	N.A. (2.8)[b,c]
C_4H_{10} (**f**)	0.344[d]
$C_4H_2F_8$ (**g**)	0.0587[d]
$C_4F_8Cl_2$ (**h**)	N.A. (N.D.)[b,c,e]
$C_4F_6Cl_4$ (**i**)	0.030[f]

[a] See Figure 1. [b] Reference 7. [c] N.A. = nonanesthetics; vapor pressure in parentheses. [d] Reference 48. [e] N.D. = not determined. [f] Unpublished results provided by E. I. Eger.

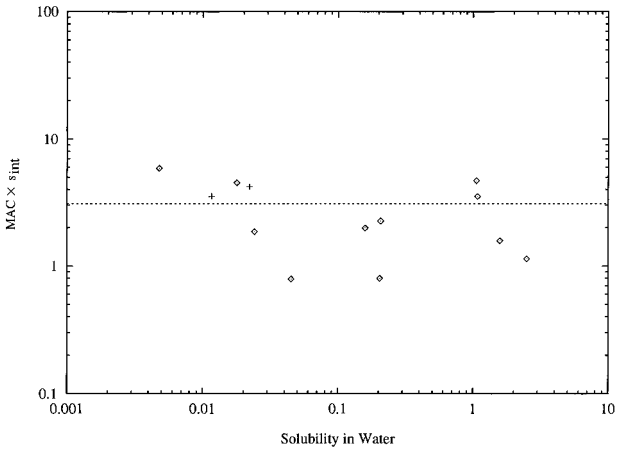

Figure 6. Product of the measured anesthetic partial pressure, MAC, and the calculated interfacial solubility *versus* the solubility in water. The compounds and the symbols are the same as in Figure 5.

The "interfacial" Meyer−Overton hypothesis for the same suite of molecules is shown in Figure 6. Here, z_1 and z_2 were set to −4 and 4 Å (the interface is at $z = 0$). These values minimize the root-mean-squares deviation of MAC × s_{int} from a constant. For easy comparison with Figure 5, C was chosen such that the average values of MAC × s_{int} and MAC × s_{oil} are both equal to 3.1. We observe that agreement with the interfacial Meyer−Overton relationship is very good for *all* molecules, including the transitional compounds. The least-squares deviation is equal to 1.5. By comparison, the deviation from the conventional Meyer−Overton relationship, excluding the transitional compounds, is 1.95. The results are not sensitive to the exact choice of the interfacial range $[z_1,z_2]$. For $[z_1,z_2]$ equal [−6,6], [−3,6], and [−6,3] Å, the root-mean-squares deviations of MAC × s_{int} from a constant differ from the minimized deviation by less than 5%.

The interfacial Meyer−Overton relationship was also tested for the same molecules at the interface between water and a simple membrane.[12,13,54] The results are equally accurate. Again, no deviation from the relationship was observed for the transitional compounds. Recently, the study of interfacial properties of anesthetics was extended to alcohols: methanol, ethanol, butanol, and hexanol.[55] These molecules deviate from the conventional Meyer−Overton relationship oppositely than transitional compounds—they are more potent than predicted from the relationship. In contrast, the product of MAC × s_{int} for these molecules is approximately the same as for other compounds studied so far. This extends the range of applicability of the interfacial Meyer−Overton relationship by another 2 orders of magnitude in anesthetic potency and 3 orders of magnitude in solubilities in water.

The constant value of MAC × s_{int} for different compounds implies that their concentrations at the water−hexane interface are the same at the anesthetic partial pressure. If the interfacial region spans the range $-4 < z < 4$ Å, the interfacial concentration of an anesthetic is 1 molecule per 200 Å^2. At this concentration, solute−solute interactions are expected to be weak, and the infinite dilution approximation used to calculate the free energy profiles is justified.

The Meyer−Overton hypothesis implies that anesthetics suppress movement by acting in the interior of neuronal membranes. However, this hypothesis fails to explain why some nonpolar anesthetics are less potent whereas highly polar anesthetics are more potent than predicted from their solubilities in oil. A good correlation between anesthetic potency and interfacial solubility points to an alternative site of action of inhaled anesthetics—an interface separating water from a nonpolar environment. This might be a water−membrane interface or the surface of a water-exposed portion of a protein receptor.

Probably the earliest suggestion of an interfacial site of anesthetic action is due to Pauling[56] and Miller,[57] who proposed that anesthesia was due to the formation of hydrate crystals around nonpolar anesthetic molecules, immobilizing surrounding water and sidechains of receptors. It is, however, unlikely that this hypothesis is correct.[58] More recent arguments for an interfacial mechanism of anesthetic action[59] are based on NMR studies exploring the distribution of general anesthetics across the water−membrane and water−micelles systems and their effect on membrane ordering. Some of these studies indicate strong preferences toward the interfacial location of anesthetics[60−63] whereas other suggest broad distributions across the membrane with only a slight preference for the lipid surface.[58,64]

Even if the site of anesthesia is identified as being located near the water−membrane interface, the mechanism by which a broad range of anesthetics, with disparate structures, exert their action at similar concentrations remains unknown. Most likely, anesthetics act on a yet to be identified membrane receptor. Current theories favor the $GABA_A$ receptor[65−67] but other membrane proteins,[68] such as glutamate receptors,[69] cannot be excluded. Anesthetics might act directly on a receptor or influence its action indirectly, for example by impeding access of an ion to an ion channel or by changing the membrane surface potential that, in turn, might modulate voltage-dependent conformational transitions in membrane receptors.[70]

A satisfactory hypothesis for the site of anesthesia should not only account for the relation between the potency of anesthetics and their free energy of binding to this site but also explain the lack of action of nonanesthetics. This is exactly where the Meyer−Overton hypothesis clearly fails, since most nonanesthetics are predicted to have an immobilizing effect. According to the interfacial hypothesis of anesthetic action, nonanesthetics should be distinguished from anesthetics by their inability to reach sufficient interfacial concentrations at any partial pressure. In some instances, such as perfluoropentane (not studied here), this is clearly the case. The results, however, are less convincing for the nonanesthetics studied in this work. Although the product of their maximum achievable partial pressures and the interfacial solubility is always smaller than the average MAC × s_{int} for the anesthetics, the difference between these two quantities is of a similar order as the fluctuations in MAC × s_{int} from its average value. Thus, an unambiguous explanation for the lack of action of nonanesthetics cannot be reached from a simple model of solute molecules interacting with the water−hexane interface.

Conclusion

In this paper, we test the hypothesis that the potency of anesthetics correlates with their solubility at an interface between water and a nonpolar phase. This idea constitutes an alternative to the Meyer−Overton hypothesis, which predicts a correlation between the anesthetic potency and the solubility in a lipidlike phase. Including previously studied compounds, 16 solutes have been examined. They belong to four series, each containing structurally similar molecules that range from potent anesthetics to nonanesthetics. For each molecule, a free energy profile was obtained across the water−hexane interface from molecular dynamics simulations. From these profiles, interfacial solubilities were calculated. The proposed correlation is obeyed by all anesthetics, even though their potencies and solubilities in water vary by 4 orders of magnitude. The correlation even holds

in the case of solutes for which the Meyer−Overton hypothesis fails. Recently, its range of applicability was extended to alcohols,[55] the anesthetic potency of which is not very well predicted by the Meyer−Overton hypothesis. Studies on several clinical anesthetics are currently in progress.[55] Furthermore, the correlation with anesthetic potency is equally good if interfacial solubilities are calculated at an interface between water and the glycerol 1-monooleate bilayer rather than the water−hexane interface.[54] A subsequent step will be to test the same correlation using solubilities at an interface between water and a phospholipid bilayer.

Whereas the conventional Meyer−Overton hypothesis implies that anesthetics act in the membrane interior, the correlation between anesthetic potency and interfacial solubility points instead to an interfacial site of anesthetic action. It is natural to propose that this site be located near the surface of the neuronal membrane, although a water-exposed surface of a protein receptor cannot be excluded. The exact nature of this site and the mechanism by which anesthetics act at the site remain unknown.

From the observed correlation, we conclude that the interfacial concentrations, at anesthetizing partial pressures, are the same for all anesthetics, irrespective of their molecular structure. Thus, potent anesthetics are characterized by higher interfacial solubilities. This is possible because the free energy profiles across the interface for many of these compounds exhibit interfacial minima. Such minima arise from a competition between the quasi-static work of forming a cavity sufficient to accommodate the solute, which is smaller in a nonpolar phase than in water, and the free energy contribution from solute−solvent interactions, which is usually more favorable in water.

The interest in the free energy profiles characterizing the transfer of these molecules across the water surface and interfaces between water and nonpolar liquids extends beyond anesthesia to many other fields as different as atmospheric chemistry and pharmacology. For example, many halogenated hydrocarbons are pollutants that participate in the destruction of the ozone layer by accumulating and undergoing reactions on surfaces of water droplets in clouds. In another example, the knowledge of free energy profiles for drugs crossing the water−membrane interface is essential for determining their bioavailability.

Acknowledgment. This work was supported by the NIH Grant GM47818-01. C.C. was supported by a National Research Council Associateship. Computer resources were provided in part by the National Cancer Institute Frederick Biomedical Supercomputer Center. We thank Drs. A. D. King, Jr., and B. A. Pethica for discussions about measuring surface excess concentrations and sharing their experimental results with us.

References and Notes

(1) Meyer, H. *Arch. Exp. Pathol. Pharmakol.* **1989**, *42*, 109.

(2) Overton, E. *Studien über die Narkose zugleich ein Betrag zur Allgemeinen Pharmakologie*; Verlag von Gustav Fischer: Jena, 1901.

(3) Chortkoff, B. S.; Laster, M. J.; Koblin, D. D.; Taheri, S.; Eger, E. I.; Halsey, M. J. *Anesth. Analg.* (*N.Y.*) **1994**, *79*, 234.

(4) Koblin, D. D. In *Anesthesia*; Miller, R., Ed.; Churchill-Livingston: New York, 1990; p 51.

(5) Janoff, A. S.; Miller, K. W. In *Biological Membranes*; Chapman, D., Ed.; Academic Press: New York, 1982; Vol. 4, p 417.

(6) These compounds do not suppress movement in response to a noxious stimulus. However, at least some of them produce another effect characteristic to all anesthetics−amnesia. Thus, more precisely, they should be called nonimmobilizers.

(7) Koblin, D. D.; Chortkoff, B. S.; Laster, M. J.; Eger, E. I.; Halsey, M. J.; Ionescu, P. *Anesth. Analg.* (*N.Y.*) **1994**, *79*, 1043.

(8) Liu, J.; Laster, M. J.; Koblin, D. D.; Eger, E. I.; Halsey, M. J.; Taheri, A.; Chortkoff, B. S. *Anesth. Analg.* (*N.Y.*) **1994**, *79*, 238.

(9) Kandel, L.; Chortkoff, B. S.; Sonner, J.; Laster, M. J.; Eger, E. I. *Anesth. Analg.* (*N.Y.*), in press.

(10) Fang, Z.; Ionescu, P.; Chortkoff, B. S.; Kandel, L.; Sonner, J.; Laster, M. J.; Eger, E. I. *Anesth. Analg.* (*N.Y.*), submitted.

(11) Both the (*S,S*)- and (*S,R*)-enantiomers were studied at the surface of water and hexane. Since the calculated and the measured solubilities as well as anesthetic potencies of these isomers are nearly identical, only the (*S,R*) enantiomer was studied in the water−hexane system.

(12) Pohorille, A.; Wilson, M. A. *J. Chem. Phys.* **1996**, *104*, 3760.

(13) Pohorille, A.; Cieplak, P.; Wilson, M. A. *Chem. Phys.* **1996**, *204*, 337.

(14) Jorgensen, W. L.; Chandrasekhar, J.; Madura, J. D.; Impey, R. W.; Klein, M. L. *J. Chem. Phys.* **1983**, *79*, 926.

(15) Jorgensen, W. L.; Madura, J. D.; Swenson, C. J. *J. Am. Chem. Soc.* **1984**, *106*, 6683.

(16) Jorgensen, W. L.; Tirado-Rives, J. *J. Am. Chem. Soc.* **1988**, *110*, 1657.

(17) Ryckaert, J.; Cicotti, G.; Berendsen, H. J. C. *J. Comput. Phys.* **1977**, *23*, 327.

(18) Van Gunsteren, W. F.; Berendsen, H. J. C. *Mol. Phys.* **1977**, *34*, 1311.

(19) Weiner, S. J.; Kollman, P. A.; Nguyen, D. T.; Case, D. A. *J. Comput. Chem.* **1986**, *7*, 230.

(20) Cornell, W. D.; Cieplak, P.; Bayly, C. I.; Gould, I. R.; Merz Jr., K. M.; Ferguson, D. M.; Spellmeyer, D. C.; Fox, T.; Caldwell, J. C.; Kollman, P. A. *J. Am. Chem. Soc.* **1995**, *117*, 5179.

(21) Pohorille, A.; Wilson, M. A. Unpublished results.

(22) Widom, B. *J. Chem. Phys.* **1963**, *39*, 2808.

(23) Gough, C. A.; Pearlman, D. A.; Kollman, P. A. *J. Comput. Chem.* **1992**, *13*, 963.

(24) Van Buuren, A. R.; Marrink, S. J.; Berendsen, H. J. C. *J. Phys. Chem.* **1993**, *97*, 9206.

(25) Marrink, S. J.; Berendsen, H. J. C. *J. Phys. Chem.* **1994**, *98*, 4155.

(26) Andzelm, J.; Wimmer, E. J. *J. Chem. Phys.* **1992**, *96*, 1280.

(27) Godbout, N.; Salahub, D. R.; Andzelm, J.; Wimmer, E. *Can. J. Chem.* **1992**, *70*, 560.

(28) Frisch, M. J.; Trucks, G. W.; Schlegel, H. B.; Gill, P. M. W.; Johnson, B. G.; Wong, M. W.; Foresman, J. B.; Robb, M. B.; Head-Gordon, M.; Replogle, E. S.; Gomperts, R.; Andres, J. L.; Raghavachari, K.; Binkley, J. S.; Gonzalez, C.; Martin, R. L.; Fox, D. J.; Defrees, D. J.; Baker, J.; Stewart, J. J. P.; Pople, J. A. *GAUSSIAN 92/DFT*; Gaussian Inc.: Pittsburgh, PA, 1993.

(29) Becke, A. D. *Phys. Rev. A* **1988**, *38*, 3098.

(30) Perdew, J. P. *Phys. Rev. A* **1986**, *33*, 8822.

(31) Rashin, A. A.; Bukatin, M. A.; Andzelm, J.; Hagler, A. T. *Biophys. Chem.* **1994**, *51*, 375.

(32) Chipot, C.; Ángyán, J. G. GRID *Version 3.0: Point Multipoles Derived From Molecular Electrostatic Properties*, QCPE No. 655, 1995.

(33) Reynolds, C. A.; Essex, J. W.; Richards, W. G. *J. Am. Chem. Soc.* **1992**, *114*, 9075.

(34) Hehre, W. J.; Radom, L.; Schleyer, P.v.R.; Pople, J. A. *Ab Initio Molecular Orbital Theory*; Wiley: New York, 1986.

(35) Chipot, C.; Ángyán, J. G.; Ferenczy, G. G.; Scheraga, H. A. *J. Phys. Chem.* **1993**, *97*, 6628.

(36) Ángyán, J. G.; Chipot, C. *Int. J. Quantum Chem.* **1994**, *52*, 17.

(37) Verlet, L. *Phys. Rev.* **1967**, *159*, 98.

(38) Owenson, B.; Pohorille, A. COSMOS−*A software package for COmputer Simulations of MOlecular Systems.* NASA−Ames Research Center, Moffett Field, CA 94035−1000, 1987.

(39) Wilson, M.; Pohorille, A. *J. Am. Chem. Soc.* **1994**, *116*, 1490.

(40) Andrea, T. A.; Swope, W. C.; Andersen, H. C. *J. Chem. Phys.* **1983**, *79*, 4576.

(41) Torrie, G. M.; Valleau, J. P. *Chem. Phys. Lett.* **1974**, *28*, 578.

(42) Bennett, C. H. *J. Comput. Phys.* **1976**, *22*, 245.

(43) Torrie, G. M.; Valleau, J. P. *J. Chem. Phys.* **1977**, *66*, 1402.

(44) Kumar, S.; Bouzida, D.; Swendsen, R. H.; Kollman, P. A.; Rosenberg, J. M. *J. Comput. Chem.* **1992**, *13*, 1011.

(45) Allen, M. P.; Tildesley, D. J. *Computer Simulation of Liquids*; Clarendon Press: Oxford, 1987.

(46) Ionescu, P.; Eger, E. I. Unpublished results, 1996.

(47) Pohorille, A.; Pratt, L. R. *J. Am. Chem. Soc.* **1990**, *112*, 5066.

(48) The free energy curves were positioned on the energy scale such that the end points would correspond to the calculated free energies of solvation in water and hexane. This was not exactly possible if the free energy of transfer from water to hexane calculated directly (column 6 in Table 3) and from individual free energies of solvation (column 8 in Table 3) were not the same. Then the difference was equally divided between both end points.

(49) Wilson, M.; Pohorille, A.; Pratt, L. R. *J. Phys. Chem.* **1987**, *91*, 4873.

(50) Goh, M. C.; Hicks, J. M.; Kenmitz, K.; Pinto, G. R.; Bhattacharrya, K. *J. Phys. Chem.* **1988**, *92*, 5074.

(51) Du, Q.; Freysz, E.; Shen, R. *Science* **1994**, *26*, 207.

(52) Pohorille, A.; Wilson, M. A. In *Reaction Dynamics in Clusters and Condensed Phases—The Jerusalem Symposia on Quantum Chemistry and Biochemistry*; Jortner, J., Levine, R., Pullman, B.; Eds.; Kluwer: Dordrecht, 1993; Vol. 26, p 207.
(53) Eger, E. I.; Liu, J.; Koblin, D. D.; Laster, M. J.; Taheri, S.; Halsey, M. J.; Ionescu, P.; Chortkoff, B. S.; Hudlicky, T. *Anesth. Analg.* (*N.Y.*) **1994**, *79*, 245.
(54) Wilson, M. A.; Chipot, C.; Pohorille, A.; Eger, E. I. *J. Phys. Chem.*, to be submitted.
(55) Pohorille, A.; Wilson, M. A.; Chipot, C. In *Progress in Colloid and Polymer Science*; Texter, J., Ed.; Springer: New York, in press.
(56) Pauling, L. *Science* **1961**, *134*, 15.
(57) Miller, S. L. *Proc. Natl. Acad. Sci. U.S.A.* **1961**, *47*, 1515.
(58) Trudell, J. R.; Hubbell, W. L. *Anesthesiology* **1976**, *44*, 202.
(59) Yoshino, A.; Murate, K.; Yosida, T.; Okabayashi, H.; Krishna, P. R.; Kamaya, H.; Ueda, I. *J. Colloid Interface Sci.* **1994**, *166*, 375.
(60) Kaneshina, S.; Lin, H. C.; Ueda, I. *Biochim. Biophys. Acta* **1981**, *647*, 223.
(61) Forrest, B. J.; Mattai, J. *Biochemistry* **1985**, *24*, 7148.
(62) Yoshino, A.; Yoshida, T.; Takahashi, K.; Ueda, I. *J. Colloid Interface Sci.* **1989**, *133*, 390.
(63) Yoshida, T.; Takahashi, K.; Ueda, I. *Biochim. Biophys. Acta* **1989**, *985*, 331.
(64) Baber, J.; Ellena, J. F.; Cafiso, D. S. *Biochemistry* **1995**, *34*, 6533.
(65) Franks, N. P.; Lieb, W. R. *Nature* **1994**, *367*, 807.
(66) Tanelian, D.; Kosek, P.; Mody, M.; MacIver, M. *Anesthesiology* **1993**, *78*, 757.
(67) Mihic, S. J.; McQuilkin, S. J.; Eger, E. I.; Ionescu, P.; Harris, R. A. *Mol. Pharmacol.* **1994**, *46*, 851.
(68) Harris, R. A.; Mihic, S. J.; Dildy-Mayfield, J. E.; Machu, T. K. *FASEB J.* **1995**, *9*, 1454.
(69) Dildy-Mayfield, J. E.; Eger, E. I.; Harris, R. A. *J. Pharmacol. Exp. Ther.* **1996**, *276*, 159.
(70) Qin, Z. H.; Szabo, G.; Cafiso, D. S. *Biochemistry* **1995**, *34*, 5536.